

Direct instantaneous power control of doubly-fed induction generator with constant switching frequency for wind energy conversion systems

Mohammad Pichan¹, Hasan Rastegar¹, Seyed Mojtaba Tabatabaei², Mohammad Monfared³

¹ Department of Electrical Engineering, Amirkabir university of Technology, Tehran, Iran

² Department of Electrical Engineering, Islamic Azad university of Najafabad, Isfahan, Iran

³ Department of Electrical Engineering, Ferdowsi University of Mashhad, Mashhad, Iran

m_pichan@yahoo.com

Abstract: This paper proposes a new method for direct power control (DPC) of a doubly-fed induction generator (DFIG)-based wind energy conversion systems. In this method, the hysteresis comparator and the switching look-up table of conventional DPC are replaced by a PWM modulator. The rotor control voltages are calculated in any sampling period directly using the measured stator voltage, references and measured active and reactive powers, rotor position and some machine parameters. The proposed method does not require any rotor current decoupling or PI controller. The converter switching frequency is constant which simplifies the design of a converters and a harmonics filter. Simulation results of a 2 MW DFIG system confirm the superior performance of the proposed control strategy.

[Pichan M, Rastegar H, Tabatabaei S.M, Monfared M. **Direct instantaneous power control of doubly-fed induction generator with constant switching frequency for wind energy conversion systems.** *J Am Sci* 2013;9(6):665-673]. (ISSN: 1545-1003). <http://www.jofamericanscience.org>. 85

Keywords: Doubly-fed induction generator, direct power control, wind energy conversion systems

1. Introduction

With ever increasing concerns about the world's fossil fuel reserves as well as CO₂ emissions, renewable energy sources, especially wind power, have found more attentions. Indeed, wind energy has become an important source for electricity generation in many countries [1]. It is expected that wind energy will provide about 10% of the world's electrical energy in 2020.

Nowadays, many wind farms are based on a doubly-fed induction generator (DFIG) technology with converters rated at 20%-30% of the generator rating. Compared to the fixed speed induction generators, the DFIG-based wind turbines, offer a lot of advantages: 1) variable speed operation which allows extracting maximum power from the wind, 2) four-quadrant converter topology which lets decoupled and fast control of active and reactive powers and improves the power quality and stability of the wind turbine, 3) reduced mechanical stresses, and 4) no need for capacitor bank to compensate for the reactive power consumed by the fixed speed induction generators [2-4]. On the other hand, compared to fully variable speed wind generation systems with a full-rated converter, DFIG systems significantly reduce the converter's costs and losses. The main drawback associated with the DFIG is slip rings used for rotor windings connections. A schematic of a DFIG-based wind energy generation system is shown in Figure 1.

The conventional technique of controlling a DFIG system is based on the rotor current vector

control, implemented through the d-q components decomposition [2, 5, 6]. This technique is performed in the synchronous reference frame aligned to the stator's voltage [5] or flux [6]. Consequently, it suffers from a lot of transformations of control outputs and inputs among reference frames which results in a complicated control system and requires numerous calculations. Another disadvantage of this method is that it is not robust against machine parameters mismatches. Furthermore, because of electromagnetic coupling between direct (d) and quadrature (q) components, it is hard to tune the rotor current controllers to ensure system stability and a desired response within the entire operating range [7, 8].

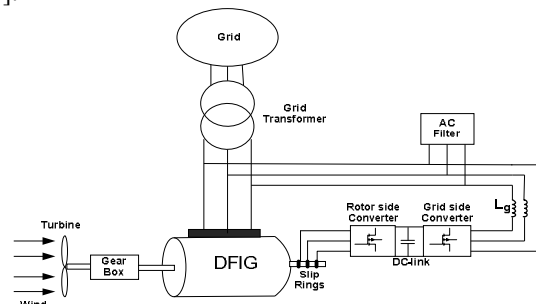


Figure 1. Schematic of a DFIG-based wind energy conversion system

Direct torque control (DTC) as an alternative for the vector control of induction machines was first introduced in the middle of 1980s [9, 10]. It has a much simpler structure than the vector control and requires less machine parameters.

One of the main problems of the DTC method is its weak performance during start-up and very low speed operation [11]. Several alternatives have been proposed to obviate this problem such as using additional trigger signal [12], modified switching table to use all available voltage vectors in each sequence [13] and predictive methods [14]. Another major problem is the variable converter switching frequency, which is a consequent of using hysteresis. The hysteresis controller bandwidth should be properly selected to ensure that the maximum allowed converter switching frequency is not exceeded [15].

Based on the DTC technique, the direct power control (DPC) was proposed for three phase pulse width modulated (PWM) converters and proven to have many advantages compared to the vector control technique, such as simplicity, fast dynamics and robustness against parameters variations and grid disturbances [16-19]. Recently, the DPC is proposed for the control of ac motors [20] and more recently DFIG [21-23]. In [21], the converter switching states are selected from a switching table, based on the active and reactive power errors and the stator flux position. Although this technique is simple and robust against the parameters variations, the converter switching frequency widely varies as a function of variations of active and reactive powers, machine speed and hysteresis bandwidth. Some solutions have been proposed to fix the converter switching frequency in [22-24] but there are some problems in these methods. In [22], there are several complex and time consuming computations which make the control algorithm too complicated for practical implementation. Also, in [23], additional measurement and transformation are needed for rotor current which increase the overall cost and complexity. Furthermore, these methods require estimating stator flux which needs additional calculation.

In this paper, a new method for direct power control of DFIG is suggested. In this method, the required rotor control voltages in each sampling period are directly calculated based on only the stator voltage, reference and measured active and reactive powers and some machine parameters. Then these control voltages are fed to a PWM modulator to generate gate pulses for the rotor side converter.

2. Conventional DPC strategy for DFIG

As expressed in [21] in detail, the active and reactive power in the synchronous reference frame can be given as:

$$P_s = K_s w_s |j_s| |j_r| \sin q \quad (1)$$

$$Q_s = -K_s w_s |j_s| (|j_r| \cos q - \frac{L_r}{L_m} j_s) \quad (2)$$

Where $L_s = L_{ds} + L_m$, $L_r = L_{dr} + L_m$,

$K_s = 1.5L_m / \sigma L_s L_r$ and θ is the angle between the stator and rotor flux vectors. Differentiating (1) and (2) with respect to time results in the following equations.

$$\frac{dP_s}{dt} = K_s w_s |j_s| \frac{d(|j_r| \sin q)}{dt} \quad (3)$$

$$\frac{dQ_s}{dt} = -K_s w_s |j_s| \frac{d(|j_r| \cos q)}{dt} \quad (4)$$

According to (3) and (4) and assuming that $|j_s|$ and ω_s remain constant, it is concluded that a fast and decoupled control of active and reactive powers is possible by regulating the rotor flux components $|j_r| \sin q$ and $|j_r| \cos q$, respectively.

The rotor flux vector can be expressed as

$$\frac{dj_r^r}{dt} = V_r^r - R_r I_r^r \quad (5)$$

Neglecting the rotor resistance effect, (5) implies that the rotor flux vector variation is directly controlled by the applied rotor voltage vector. The rotor flux vector is in the same direction as the rotor voltage vector and its speed is proportional to the amplitude of the applied voltage vector. For a two-level converter with six switches, eight possible voltage vectors (six active and two zero voltage vectors) are expected [18]. Knowing the stator flux position, the impact of each voltage vector on the rotor flux, and consequently on $|j_r| \sin q$ and $|j_r| \cos q$ components, can be readily determined. Therefore, according to (3) and (4), the effect of each voltage vector on the active and reactive power changes can be evaluated and the proper switching table can be determined to give the most effective rotor voltage vector in each sampling instance to minimize the power errors [21].

Figure 2. shows the schematic diagram of the conventional DPC control strategy for the DFIG system. In order to achieve an accurate power control with minimum current distortion, the sampling frequency must be sufficiently high, usually in the range of tens of kHz which can increase the EMI noises and the implementation difficulties. The converter switching frequency can significantly vary with the variations of the operating conditions, such as active and reactive powers or rotor slip variations. So, it is difficult to calculate the converter losses in order to design the cooling system. In addition, the

AC filter which prevents penetrating the current harmonics into the grid has a complicated design, since it has to absorb a wide range of frequency components without the probability of any resonances. Furthermore, under distorted grid voltages, the estimation of the stator flux requires complicated algorithms with increased computational burden.

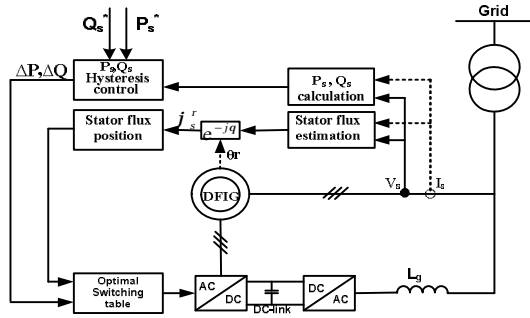


Figure 2. Schematic diagram of the conventional DPC

3. Proposed DPC strategy

3.1. Model of DFIG in the synchronous reference frame

The stator and rotor voltage equations in the synchronous reference frame are as

$$V_s^s = R_s I_s^s + \frac{dj_s^s}{dt} + j\omega_s j_s^s \quad (6)$$

$$V_r^s = R_r I_r^s + \frac{dj_r^s}{dt} + j(\omega_s - \omega_r) j_r^s \quad (7)$$

where $\omega_{slip} = \omega_s - \omega_r$ is the slip angular frequency. The stator and rotor flux linkages are also given by

$$j_s^s = L_s I_s^s + L_m I_r^s \quad (8)$$

$$j_r^s = L_m I_s^s + L_r I_r^s \quad (9)$$

The stator current in the synchronous reference frame can be obtained from the above equations as

$$I_s^s = \frac{L_r j_s^s - L_m j_r^s}{L_s L_r - L_m^2} = \frac{j_s^s}{s L_s} - \frac{L_m j_r^s}{s L_s L_r} \quad (10)$$

where $s = (L_s L_r - L_m^2) / L_m^2$ is the leakage factor.

The active and reactive powers injected to the grid are given by

$$P_s + jQ_s = -\frac{3}{2} V_s^s \times I_s^{s*} \quad (11)$$

Under ideal grid voltages, the amplitude and rotating speed of the stator flux are constant and consequently $dj_s^s/dt = 0$. Assuming that the stator copper losses can be neglected, the stator voltage vector equation is simplified as

$$V_s^s = j\omega_s j_s^s \quad (12)$$

If, by using a PLL, the d-axis of the synchronous reference frame is aligned to the stator voltage vector, equation (12) results in

$$j_{sd}^s = 0, j_{sq}^s = -V_{sd}^s / \omega_s \quad (13)$$

Substituting (10) and (13) in (11), the stator active and reactive powers are calculated as

$$P_s + jQ_s = -\frac{3}{2} V_{sd}^s \left(\frac{j_{sd}^s}{s L_s} - \frac{L_m j_{rd}^s}{s L_s L_r} \right) = -\frac{3}{2} V_{sd}^s \left(j \frac{V_{sd}^s}{\omega_s} - \frac{L_m}{L_r} (j_{rd}^s - j j_{rq}^s) \right) \quad (14)$$

Equation (14) is decomposed into the real and imaginary components to achieve the active and reactive powers.

$$P_s = K_s V_{sd}^s j_{rd}^s \quad (15)$$

$$Q_s = -K_s V_{sd}^s \left(\frac{L_r}{L_m} \frac{V_{sd}^s}{\omega_s} + j_{rq}^s \right) \quad (16)$$

Since under balanced grid conditions, the stator voltage amplitude remains constant, the power equations of (15) and (16) imply that the active and reactive powers injected to the grid can be effectively controlled by regulating the rotor flux components φ_{rd} and φ_{rq} , respectively.

3.2. Active and reactive powers control by adjusting the rotor flux vector

Equation (7) is rearranged and discretized in each small sampling period T_s as follow

$$\frac{dj_r^s}{dt} = \frac{j_r^s(k+1) - j_r^s(k)}{T_s} = V_r^s(k) - R_r I_r^s(k) - j(\omega_s - \omega_r) j_r^s(k) \quad (17)$$

$$V_r^s(k) - R_r I_r^s(k) - j(\omega_s - \omega_r) j_r^s(k)$$

After decomposing the above result into d and q components and neglecting the rotor resistance effect, the rotor flux components at the sampling point (k+1) are obtained as

$$j_{rd}^s(k+1) = j_{rd}^s(k) + T_s V_{rd}^s(k) + T_s (\omega_s - \omega_r) j_{rq}^s(k) \quad (18)$$

$$j_{rq}^s(k+1) = j_{rq}^s(k) + T_s V_{rq}^s(k) - T_s (\omega_s - \omega_r) j_{rd}^s(k) \quad (19)$$

Equation (15) and (16) can be updated with above fluxes to give the active and reactive powers at the sampling point (k+1).

$$P(k+1) = K_s V_{sd}^s(k) j_{rd}^s(k+1) \quad (20)$$

$$Q(k+1) = -K_s V_{sd}^s(k) \left[\frac{L_r}{L_m} \frac{V_{sd}^s(k)}{\omega_s} + j_{rq}^s(k+1) \right] \quad (21)$$

The aim of control system is to bring the active and reactive powers to the reference values which are available at the sampling point (k), i.e.

$$P(k+1) = P_{ref}^s(k) \quad (22)$$

$$Q(k+1) = Q_{ref}(k) \quad (23)$$

Substituting (18), (19), (22) and (23) into (20) and (21), the reference values for the rotor voltages in the synchronous reference frame are calculated as

$$V_{rd}(k) = \frac{P_{ref}(k) - P(k)}{T_s K_s V_{sd}(k)} + \frac{w_s - w_r}{K_s V_{sd}(k)} Q(k) + \frac{(w_s - w_r) L_r}{L_m w_s} V_{sd}(k) \quad (24)$$

$$V_{rq}(k) = -\frac{Q_{ref}(k) - Q(k)}{T_s K_s V_{sd}(k)} + \frac{w_s - w_r}{K_s V_{sd}(k)} P(k) \quad (25)$$

Obviously, the reference voltages calculations include a few multiplications and divisions which are not as complex as those presented in [22]. Also these equations are based on stator voltage not stator flux. Also, additional rotor current measurement as used in [23] is removed. There is no need for PI controllers used in vector control strategies or look-up table and hysteresis comparators used in the DTC or the conventional DPC.

3.3. Rotor voltage limitation

For a two level or other converters that can be used as the rotor side converter, the maximum output voltage is limited by the DC-link voltage and semiconductors ratings. For a DFIG, stator-rotor winding has a turn ratio so the voltage that can be applied to the rotor is usually about 30% of the stator voltage. Although under the steady-state operation, the rotor reference voltages do not exceed the rotor voltage limit, but they may go beyond the limit at transients such as fast or large changes in the power references. The developed voltages by the controller should be kept within the machine and converter limits to ensure a good transient performance. Based on (24) and (25), variations of active and reactive power references result in V_{rd} and V_{rq} variations, respectively. Once the active power reference undergoes a large change, V_{rd} may change significantly and exceed the maximum available rotor voltage. So it should be limited. In this condition, the controller will keep the V_{rq} unchanged and scale the V_{rd} according to the maximum output voltage of the rotor side converter. As a result, the reactive power remains under control while the active power moves to a value imposed by the scaled V_{rd} . So the scaled reference voltages are suggested as

$$V_{rq}' = V_{rq} \quad (26)$$

$$V_{rd}' = \text{sign}(V_{rd}) \sqrt{V_{r,max}^2 - V_{rq}^2} \quad (27)$$

$V_{r,max}$ is the maximum voltage that the rotor side converter can generate e.g. for the two-level three-leg converter it is $2VDC/3$, where VDC is the DC-link voltage. The same approach is adopted for a large change of reactive power reference. Here, V_{rd} remains unchanged and V_{rq} is scaled such that:

$$V_{rd}' = V_{rd} \quad (28)$$

$$V_{rq}' = \text{sign}(V_{rq}) \sqrt{V_{r,max}^2 - V_{rd}^2} \quad (29)$$

If both active and reactive power references change simultaneously, both V_{rd} and V_{rq} must be scaled as shown below.

$$V_{rd}' = V_{rd} \frac{V_{r,max}}{\sqrt{V_{rd}^2 + V_{rq}^2}} \quad (30)$$

$$V_{rq}' = V_{rq} \frac{V_{r,max}}{\sqrt{V_{rd}^2 + V_{rq}^2}} \quad (31)$$

Once the rotor reference voltages are calculated and scaled (if necessary), these voltages must be transformed to the rotor reference frame. This is achieved by the following equation

$$V_r^r = V_r^s e^{j(w_s - w_r)t} \quad (32)$$

The schematic diagram of the propose DPC for DFIGs is shown in Figure 3. Once V_r^r is calculated, advanced pulse width modulation techniques such as SPWM, SVPWM, etc. can be used to generate the desired voltages at a fixed switching frequency.

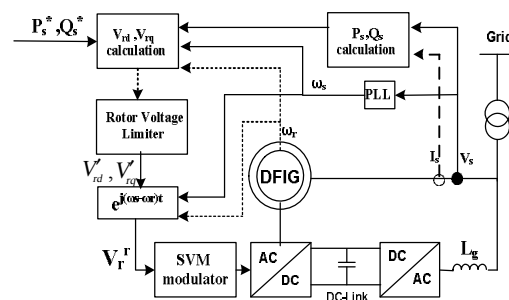


Figure 3. Schematic diagram of the proposed DPC

Compared to the conventional DPC, the switching table and hysteresis comparators are replaced by PWM modulator. Also, since the rotor reference voltages are directly calculated in the proposed method, if the power converter is changed, only the PWM modulator will be changed. This is

simpler than defining new switching table like conventional DPC.

4. Performance evaluation

To investigate the performance of the proposed control strategy under different conditions, extensive simulations are conducted using MATLAB/SIMULINK software. The simulated system is shown in Figure 4. and the system parameters are given in Table 1.

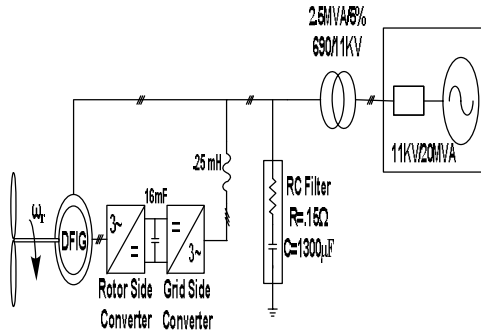


Figure 4. Configuration of the simulated system

Table 1. Parameters of simulated DFIG

Rated power	2 MW
Stator voltage	690 V
Stator/rotor turns ratio	0.3
R_s	0.0108 pu
R_r	0.0121 pu(referred to the stator)
L_m	3.362 pu
$L_{\sigma s}$	0.102 pu
$L_{\sigma r}$	0.11 pu(referred to the stator)
Lumped inertia constant	0.2 s
Number of pole pairs	2

The DFIG is rated at 2 MW. The grid side converter is responsible for balancing the power exchange between the rotor and grid through maintaining a fixed DC-link voltage. The rotor side converter is intended to control the stator active and reactive powers. The control strategy of the grid side converter is practically the same as grid-connected rectifiers [25, 26]. In this paper we used the proposed method in [25] and the DC-link voltage is adjusted at 1200 V.

A high frequency RC filter is connected to the stator side to absorb the switching harmonics and high frequency noises generated by the two converters. During the simulations, the sampling period was set to 250 μ s. To generate the switching pulses, the space vector modulation (SVM) technique with the switching frequency fixed at 2 kHz is utilized.

4.1. Steady-state and dynamic responses

The start-up procedure has three steps: 1) the grid side converter is activated to make and fix

the DC-link voltage; 2) the stator is energized at constant rotor speed; 3) the rotor side converter is activated to move the stator active and reactive powers toward the reference values. The final step is only shown in the following results and the two first steps are not displayed. The rotor speed was set externally constant, which is true because the large wind turbine inertia results in negligible speed changes. The performance of the proposed and the conventional DPC strategies in the steady-state condition is compared in Figure 5. For both strategies, the active and reactive power references are set to 2 MW and -0.5 MVar, respectively ('-' indicates absorbing the reactive power). The rotor speed is set to 0.8 pu, where the synchronous speed is defined as 1 unit. Evidently, the proposed strategy provides precise power control with minimum current distortion and less harmonic noises and at the same time, more accurate regulation and less ripples in the output active and reactive powers.

In another study, various step changes in the active and reactive power references are applied to evaluate the dynamic performance of the proposed DPC and the results are compared to those of the conventional DPC. The results for both conventional and proposed DPCs are shown in Figure 6. for rotor speed of 1 pu. Initially the rotor side converter is enabled with the active and reactive power references at 0 MW and -0.5 MVar, respectively. The active and reactive power references jumped from 0 to 2 MW at 0.2 s and from -0.5 to 0.5 MVar at 0.5 s, respectively. Then, the active power reference undergoes a fall at 0.7 s to evaluate both rising and falling performances. As one can see, the proposed control strategy has a fast dynamic response and the active and reactive powers settle to the reference values within a few milliseconds. The conventional DPC can also achieve almost the same dynamic performance. Due to the fast nature of both DPCs, a decoupled control of active and reactive powers is also achieved.

4.2. Impact of parameters mismatch

Based on (24) and (25), the only machine parameters that are used in the rotor voltage equations are k_σ and L_r / L_m ratio. Because the leakage fluxes magnetic path is mainly in the air, so the variations of the leakage inductances ($L_{\sigma s}$ and $L_{\sigma r}$) during the operation are not significant and can be safely neglected. The variations of the mutual inductance (L_m), even if large, can also be readily ignored. As described in Appendix A, the required parameters in the rotor reference voltage equations can be simplified.

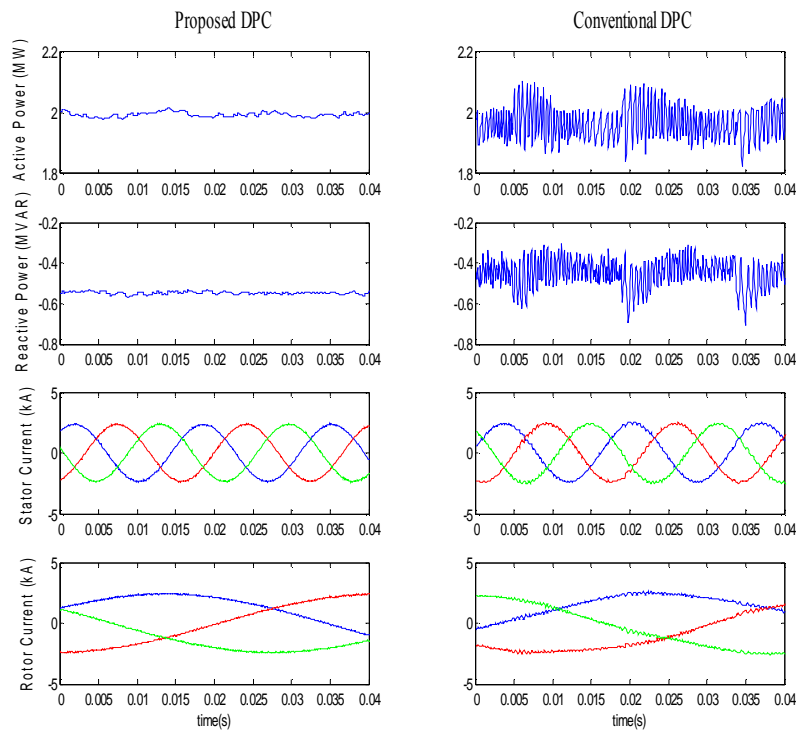


Figure 5. Steady-state operation of the proposed and conventional DPCs at rotor speed of 0.8pu

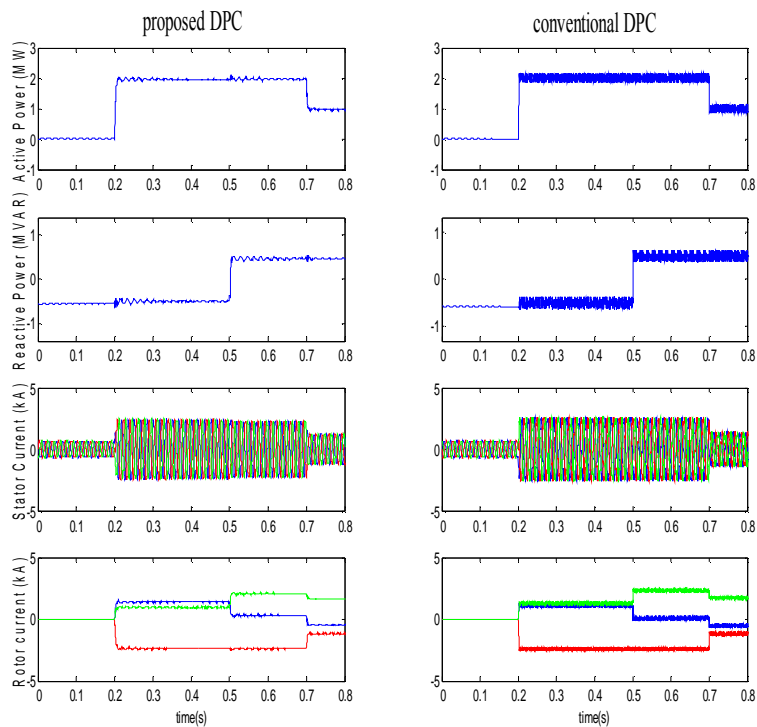


Figure 6. Transient performance of the proposed and conventional DPCs under various active and reactive power step changes at rotor speed of 1 pu.

$$k_s \approx \frac{3}{2} \frac{1}{L_{ss} + L_{sr}}, \frac{L_r}{L_m} = 1 + \frac{L_{sr}}{L_m} \approx 1 \quad (33)$$

So the impact of mutual inductance changes on the rotor reference voltages is also negligible. However, simulations are conducted to investigate the performance of the proposed DPC under mismatches in the mutual inductance value used in

the algorithm. The results are depicted in Figure 7. in which $S_{error}(\%)$ and $\Delta S(\%)$ are defined by

$$S_{error}(\%) = \sqrt{\frac{(P - P_{ref})^2 + (Q - Q_{ref})^2}{P_{ref}^2 + Q_{ref}^2}} \times 100 \quad (34)$$

$$\Delta S(\%) = \sqrt{\frac{\Delta P^2 + \Delta Q^2}{P_{ref}^2 + Q_{ref}^2}} \times 100 \quad (35)$$

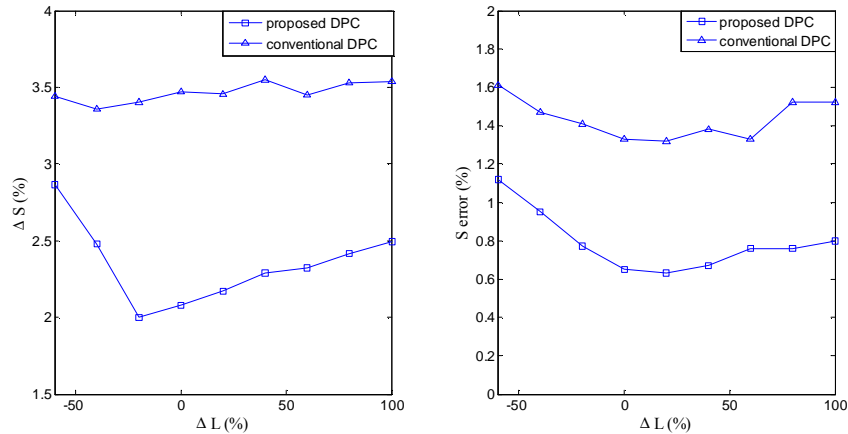


Figure 7. The effect of mutual inductance mismatch ($P_{ref} = 2$ MW, $Q_{ref} = -0.5$ MVar)

As one can see, even with large mutual inductance mismatches, the power error as well as the power ripple is very small, especially when a bigger value is used in the algorithm.

Simulation with various power steps during rotor speed variation were carried out to further test the proposed DPC scheme and the results are shown in Figure 8. Wind speed changes frequently so rotor speed variation is unavoidable. Thus the control strategy should be able to track the reference values.

According to Figure 8, it is evident that the proposed control strategy maintains its normal operation even with rotor speed changes and various power steps.

4.3. Operation under network voltage distortions

The conventional DPC technique needs to exactly estimate the stator or rotor flux vectors which may not be possible under grid voltage disturbances. On the other hand, the proposed method is also based on the measured stator voltage. This results in deteriorated performance or even instability in some cases for both conventional and proposed DPC techniques under network voltage distortions.

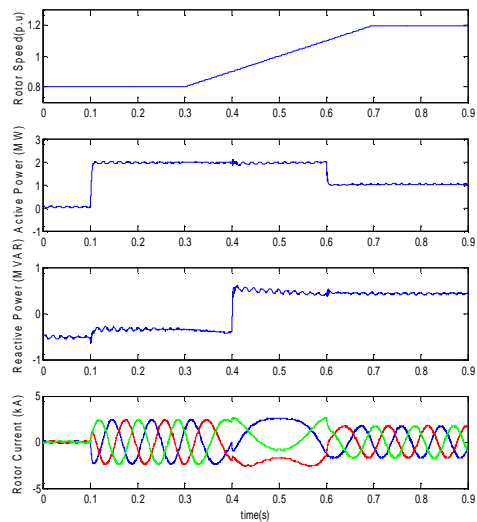


Figure 8. Simulated results under various stator active and reactive power steps and rotor speed variation.

To examine the performance of the proposed control strategy under grid voltage distortions, a simulation was done with 5th and 7th harmonic

components injected into the grid voltages, as shown in (36).

$$V_u = V_m \sin(\omega t) + k_1 V_m \sin(5\omega t) + k_2 V_m \sin(7\omega t)$$

$$V_v = V_m \sin(\omega t - \frac{2p}{3}) + k_1 V_m \sin(5\omega t + \frac{2p}{3}) + k_2 V_m \sin(7\omega t - \frac{2p}{3}) \quad (36)$$

$$V_w = V_m \sin(\omega t + \frac{2p}{3}) + k_1 V_m \sin(5\omega t - \frac{2p}{3}) + k_2 V_m \sin(7\omega t + \frac{2p}{3})$$

For different values of k_1 and k_2 , the power error and ripple are summarized in Table 2. Both control strategies maintain their normal operation, in the term of power error. Since the network voltage is harmonic distorted, the calculated powers are not constant and have a ripple which is larger in the case of the proposed DPC.

4.4. Operation under network voltage imbalance

In case of imbalanced network voltages, considering positive and negative sequence components, network voltages are defined by

$$V_{sa} = V_m \sin(\omega t) + k_3 V_m \sin(\omega t)$$

$$V_{sb} = V_m \sin(\omega t - \frac{2p}{3}) + k_3 V_m \sin(\omega t + \frac{2p}{3}) \quad (40)$$

$$V_{sc} = V_m \sin(\omega t + \frac{2p}{3}) + k_3 V_m \sin(\omega t - \frac{2p}{3})$$

Under imbalanced network voltage conditions, the quality of the PLL mainly determines the control strategy's performance. We use a simple PLL for both methods. As shown in Table 2, the imbalanced voltage mainly increases the power ripple which is more evident for the proposed technique.]

Table 2. Power error and power ripple as a function of 5th and 7th harmonic amplitudes and voltage imbalance (Pref=2 MW, Qref=-0.5 MVar)

k1	k2	k3	proposed DPC Serror(%) ΔS(%)	conventional DPC Serror(%) ΔS(%)
0	0	0	0.8 2.3766	1.02 3.19
0.03	0.01	0	0.87 7.3545	1.06 3.2015
0.05	0.03	0	1.31 11.3966	1.07 3.4215
0	0	0.01	0.87 5.6245	1.08 3.3707
0	0	0.03	0.96 8.6587	1.14 3.3992

5. Conclusion

In this paper a novel method for direct power control (DPC) of a doubly-fed induction generator (DFIG)-based wind turbine system is presented. Besides its simplicity and constant

switching frequency, the proposed DPC is robust against machine parameters mismatch. Compared to the conventional methods, the hysteresis comparators and the switching table are replaced by the PWM modulator. Also, this method doesn't require the rotor current decoupling and the PI controllers such as used in the vector control. Compared with the conventional DPC, the proposed technique provides more precise power control with less distortions and harmonic noises. Both control strategies maintain their normal operation under imbalanced and distorted grid voltages. The proposed method offers other advantages like low sampling frequency needed for digital implementation and applicable for all kind of converters.

Corresponding Author:

Mohammad Pichan
Department of Electrical Engineering
Amirkabir University of technology
Tehran, Iran
E-mail: m_pichan@yahoo.com

References

- Ahmed M.H, Bhattacharya K, Salama M. M. A. Stochastic Unit Commitment with Wind Generation Penetration," *Elect. Power Compon. Syst* 2012; 40(12): 1405–1422.
- Doncker R.W.D, Muller S, Deicke M. Doubly fed induction generator systems for wind turbines," *IEEE Ind. Appl. Mag* 2002; 8(3): 26–33.
- Okedu K.E, Muyeen S. M, Takahashi R, Tamura J. Effectiveness of Current-controlled Voltage Source Converter Excited Doubly Fed Induction Generator for Wind Farm Stabilization. *Elect. Power Compon. Syst* 2012; 40(5): 556–574.
- Fernandez L.M, Garcia C.A, Jurado F. Operating capability as a PQ/PV node of a direct-drive wind turbine based on a permanent magnet synchronous generator," *Renew. Energy* 2010; 35: 1308–1318.
- Akagi H, Sato H. Control and performance of a doubly-fed induction machine intended for a flywheel energy storage system. *IEEE Trans. Power Electron* 2002; 17(1): 109–116.
- Pena R, Clare J.C, Asher G. M. Doubly fed induction generator using back-to-back PWM converters and its application to variable-speed wind-energy generation. *Inst. Elect. Eng. Proc. Elect. Power Appl* 1996; 143(3): 231–241.
- Mohseni M, Islam S.M, Masoum M.A.S. Enhanced hysteresis-based current regulators in vector control of DFIG wind turbines. *IEEE Trans. Power Electron* 2011; 26; 1: 223–235.

8. Tremblay E, Atayde S, Chandra A. Comparative study of control strategies for the doubly fed induction generator in wind energy conversion systems: A DSP-based implementation approach. *IEEE Trans. Sustainable Energy* 2011; 2(3): 288–300.
9. Takahashi I, Noguchi T. A new quick-response and high-efficiency control strategy of an induction motor. *Inst. Elect. Eng. Trans. Ind. Appl* 1986; 22(5): 820–827.
10. Depenbrock M. Direct self-control (DSC) of inverter-fed induction machine. *IEEE Trans. Power Electron* 1988; 3(4): 420–429.
11. Buja G.S, Kazmierkowski M. P. Direct torque control of PWM inverter-fed AC motors—A survey. *IEEE Trans. Ind. Electron* 2004; 51(4): 744–757.
12. Kazmierkowski M. P, Kasprowicz A. Improved direct torque and flux vector control of PWM inverter-fed induction motor drives. *IEEE Trans. Ind. Electron* 1995; 42(4): 344–350.
13. P. Vas, Sensorless Vector and Direct Torque Control. Oxford, U.K.; Clarendon, 1998.
14. Baader U, Depenbrock M, Gierse G. Direct self-control (DSC) of inverter-fed induction machine—A basis for speed control without speed measurement. *IEEE Trans. Ind. Appl* 1992; 28(3): 581–588.
15. Casadei D, Grandi G, Serra G, Tani A. Effects of flux and torque hysteresis band amplitude in direct torque control of induction machines. in *Proc. 20th Int. Conf. Ind. Electron., Control Instrum.*, 1994, pp. 299–304.
16. Noguchi T, Tomiki H, Kondo S, Takahashi I. Direct power control of PWM converter without power-source voltage sensors. *IEEE Trans. Ind. Appl* 1998; 34(3): 473–479.
17. Escobar G, Stankovic A.M, Carrasco J.M, Galvan E, Ortega R. Analysis and design of direct power control (DPC) for a three phase synchronous rectifier via output regulation subspaces. *IEEE Trans. Power Electron* 2003; 18(3): 823–830.
18. Malinowski M, Kazmierkowski M.P, Hansen S, Blaabjerg F, Marques G.D. Virtual-flux-based direct power control of three-phase PWM rectifiers. *IEEE Trans. Ind. Appl* 2001; 37(4): 1019–1027.
19. Kazemi M.V, Yazdankhah A.S, Kojabadi H.M. Direct power control of DFIG based on discrete space vector modulation. *Renewable Energy* 2010;35(5):1033–42.
20. Luo X. Direct power control of AC motors. Master's thesis, University of Nevada, Reno, 2009.[online]. Available:\url{<http://search.proquest.com/docview/304945410/fulltextPDF/134EBD955116D8DB4AA/1?accountid=45164>}.
21. Xu L, Cartwright P. Direct active and reactive power control of DFIG for wind energy generation. *IEEE Trans. Energy Convers* 2006; 21(3):750–758.
22. Zhi D, Xu L, Williams B.W. Model-Based Predictive Direct Power Control of Doubly Fed Induction Generator. *IEEE Trans.on Power Electronics* 2010; 25(2).
23. Sguarezifilho A.J, RUPPERT E. A Deadbeat Active and Reactive Power Control for Doubly Fed Induction Generator. *Elect. Power Compon. Syst* 2012; 38(5):592–602.
24. Zhi D, Xu L. Direct Power Control of DFIG With Constant Switching Frequency and Improved Transient Performance. *IEEE Trans. Energy Convers* 2007; 22: 110–118.
25. Monfared M, Rastegar H, Kojabadi H.M. High performance direct instantaneous power control of PWM rectifiers. *Energy Conversion and Manage* 2010 (51): 947–954.
26. Ranjan K.B, Gao W. A Novel Controller Design for Grid side Converter of Doubly Fed Induction Generator for Wind Power Interface: An Experimental Investigation. *Elect. Power Compon. Syst* 2012; 38(14):1531–1544.

5/8/2013